

Supporting information

Yellow-to-brown and yellow-to-green electrochromic devices based on complexes of transition metal ions with triphenylamine- based ligand

Radosław Banasz,^{a,b} Maciej Kubicki,^a Monika Wałęsa-Chorab^{a,b*}

^a *Faculty of Chemistry, Adam Mickiewicz University in Poznań, Uniwersytetu Poznańskiego
8, 61-614 Poznań, Poland*

^b *Centre for Advanced Technologies, Adam Mickiewicz University, Uniwersytetu
Poznańskiego 10, 61-614 Poznań, Poland*

Corresponding author e-mail: mchorab@amu.edu.pl

Table of Contents

Figure S 1. FTIR spectra of ligand L (black), Fe(II) complex (red), Co(II) complex (blue) and Zn(II) complex (magenta).	3
Figure S 2. Presentation of the short contacts between the perchlorate anion and the cation complexes.	3
Figure S 3. XPS survey spectrum of ligand L (red) and its complexes with Fe(II) (green), Co(II) (blue) and Zn(II) (black) metal ions. The major XPS peaks are marked.	4
Figure S 4. CV and SWV of ligand L measured in anhydrous and deaerated 0.1 M solution of TBAClO ₄ in PC as an electrolyte at 50 mV/s scan rate.	4
Figure S 5. A) CV profiles of Fe(II) complex at different scan rates; B) Peak current vs. the square root of the scan rate for the Fe(II) complex.	5
Figure S 6. A) CV profiles of Zn(II) complex at different scan rates; B) Peak current vs. the square root of the scan rate for the Zn(II) complex.	5
Figure S 7. The UV-Vis spectra of ligand L in its neutral (black) and oxidized (red) states.	6
Figure S 8. The zoom of MLCT and LMCT bands in spectroelectrochemistry of Fe(II) complex in anhydrous and deaerated PC with 0.1 M TBAClO ₄ as a supporting electrolyte by applying potentials of 0V (■), +0.7V (■), +0.8V (■), +0.9V (■) and +1.0V (■) versus Ag/AgCl gel reference electrode held for 30 s per potential. Inset: photographs of complex Fe(II) in two different redox states.	6
Figure S 9. AFM micrographs of complex Fe(II) (A), Co(II) (B) and Zn(II) (C) spray-coated on ITO electrodes. AFM cross-section profiles were measured at a marked places.	7
Figure S 10. AFM cross-section profiles of complexes: Fe(II) (black), Co(II) (red) and Zn(II) (blue) measured at marked places.	7
Figure S11. HR-ESI-MS spectrum of Fe(II) complex.	8
Figure S12. HR-ESI-MS spectra of Co(II) complex.	8
Figure S13. HR-ESI-MS spectra of Zn(II) complex.	9
Figure S14. HR-ESI-MS spectra of ligand L	9
Figure S15. HR-ESI-MS spectra of compound A	10
Figure S16. HR-ESI-MS spectra of compound B	10
Figure S17. ¹ H NMR spectra of ligand L in d ₆ -DMSO.	11
Figure S18. ¹³ C NMR spectra of ligand L in d ₆ -DMSO.	11
Figure S19. ¹ H NMR spectra of compound A in CDCl ₃	12
Figure S20. ¹³ C NMR of compound A in CDCl ₃	12
Figure S21. ¹ H NMR spectra of compound B in CDCl ₃	13
Figure S22. ¹³ C NMR spectra of compound B in CDCl ₃	13

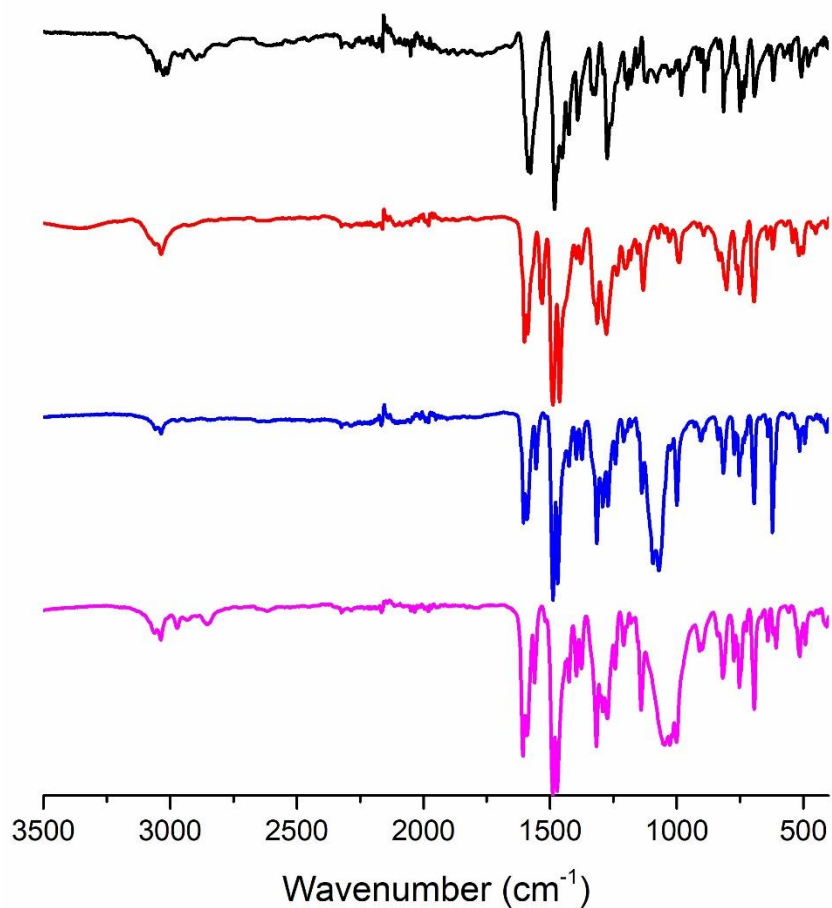


Figure S 1. FTIR spectra of ligand **L** (black), Fe(II) complex (red), Co(II) complex (blue) and Zn(II) complex (magenta).

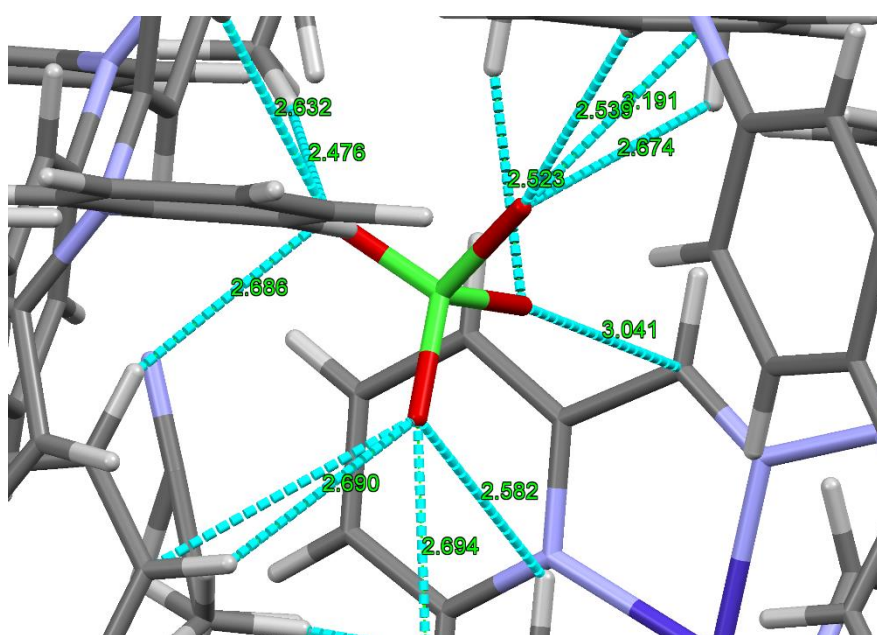


Figure S 2. Presentation of the short contacts between the perchlorate anion and the cation complexes.

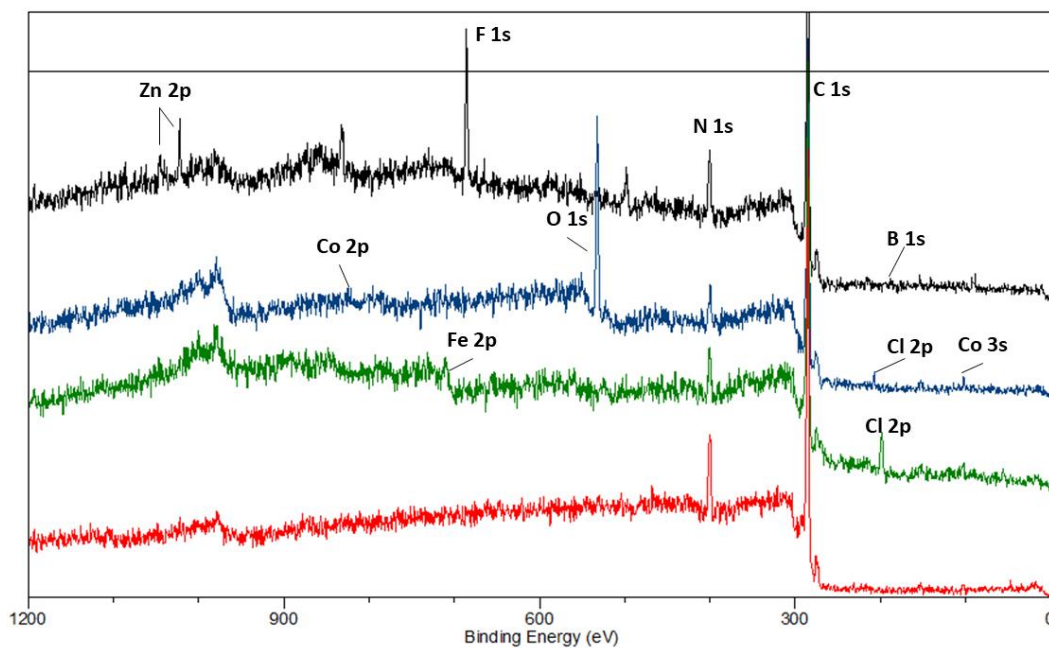


Figure S 3. XPS survey spectrum of ligand **L** (red) and its complexes with Fe(II) (green), Co(II) (blue) and Zn(II) (black) metal ions. The major XPS peaks are marked.

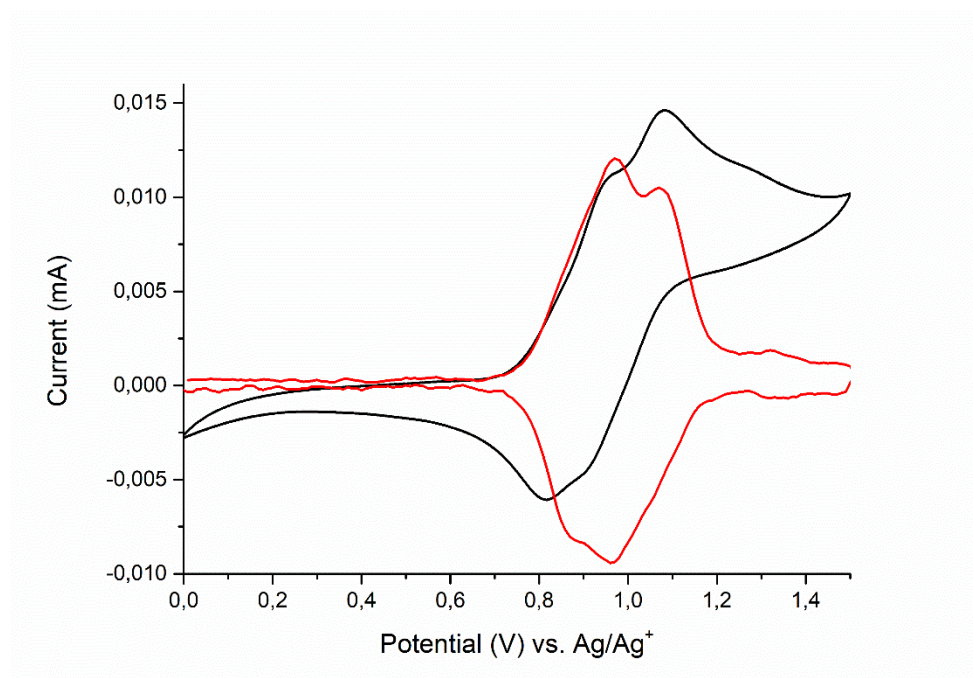


Figure S 4. CV and SWV of ligand **L** measured in anhydrous and deaerated 0.1 M solution of TBAClO₄ in PC as an electrolyte at 50 mV/s scan rate.

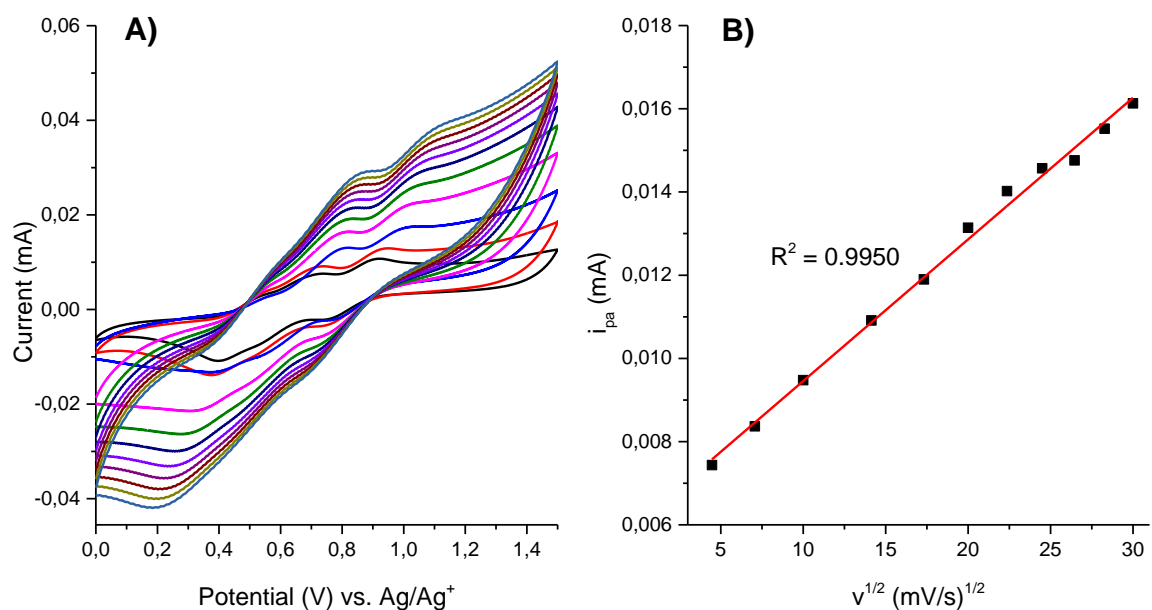


Figure S 5. A) CV profiles of Fe(II) complex at different scan rates; B) Peak current vs. the square root of the scan rate for the Fe(II) complex.

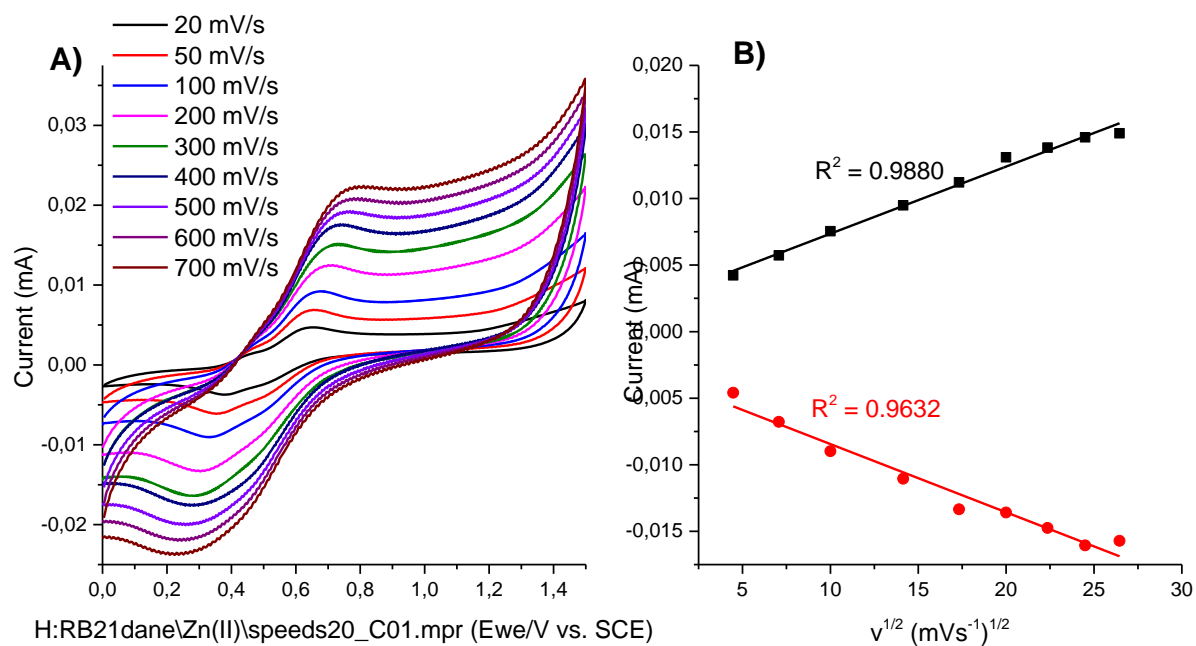


Figure S 6. A) CV profiles of Zn(II) complex at different scan rates; B) Peak current vs. the square root of the scan rate for the Zn(II) complex.

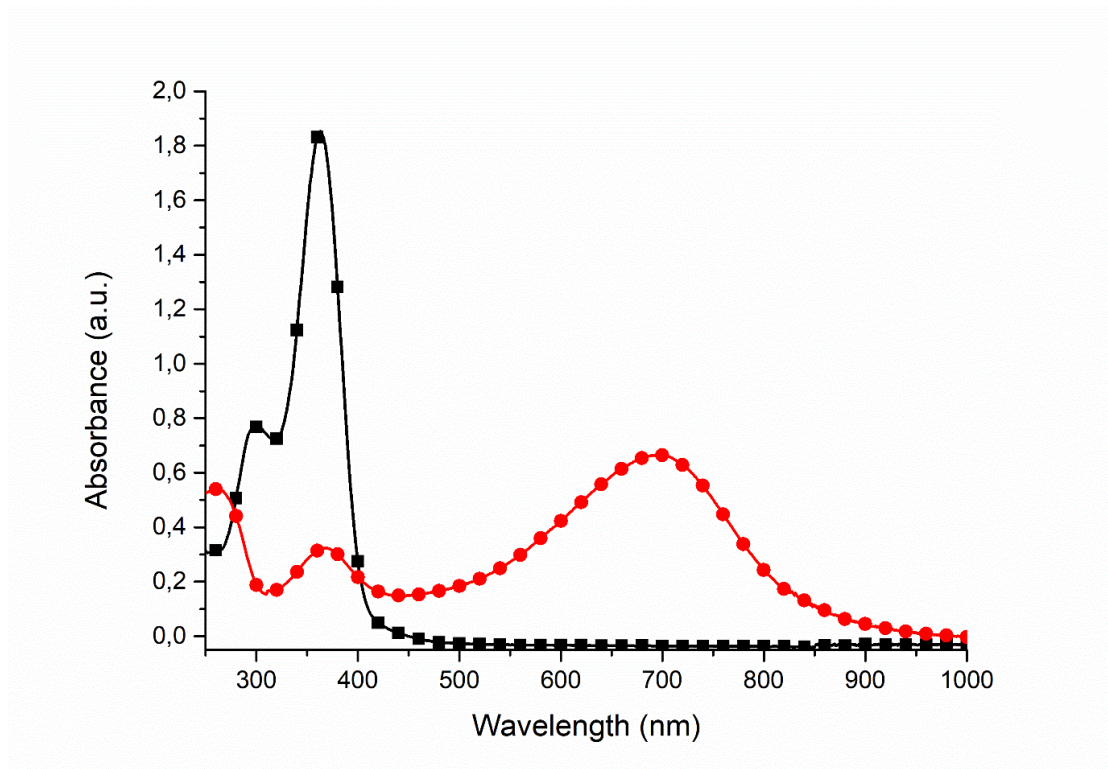


Figure S 7. The UV-Vis spectra of ligand **L** in its neutral (black) and oxidized (red) states.

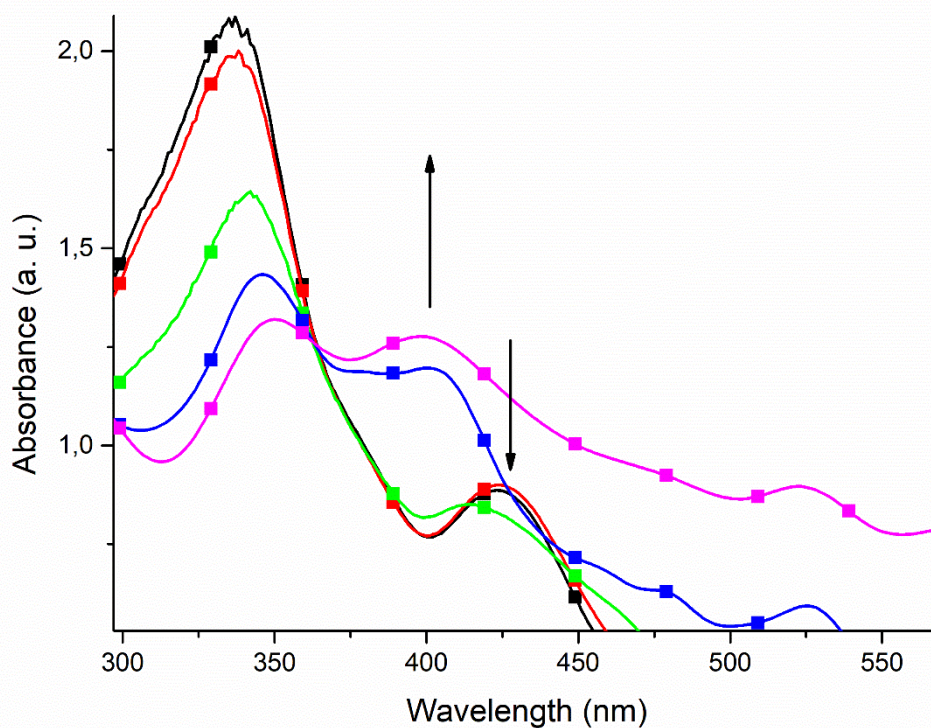


Figure S 8. The zoom of MLCT and LMCT bands in spectroelectrochemistry of Fe(II) complex in anhydrous and deaerated PC with 0.1 M TBAClO₄ as a supporting electrolyte by applying potentials of 0V (■), +0.7V (■), +0.8V (■), +0.9V (■) and +1.0V (■) versus Ag/AgCl gel

reference electrode held for 30 s per potential. Inset: photographs of complex Fe(II) in two different redox states.

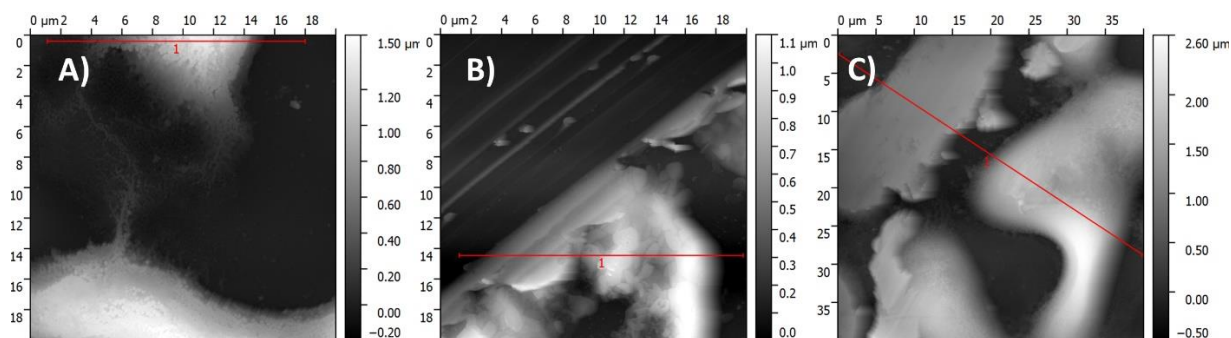


Figure S 9. AFM micrographs of complex Fe(II) (A), Co(II) (B) and Zn(II) (C) spray-coated on ITO electrodes. AFM cross-section profiles were measured at a marked places.

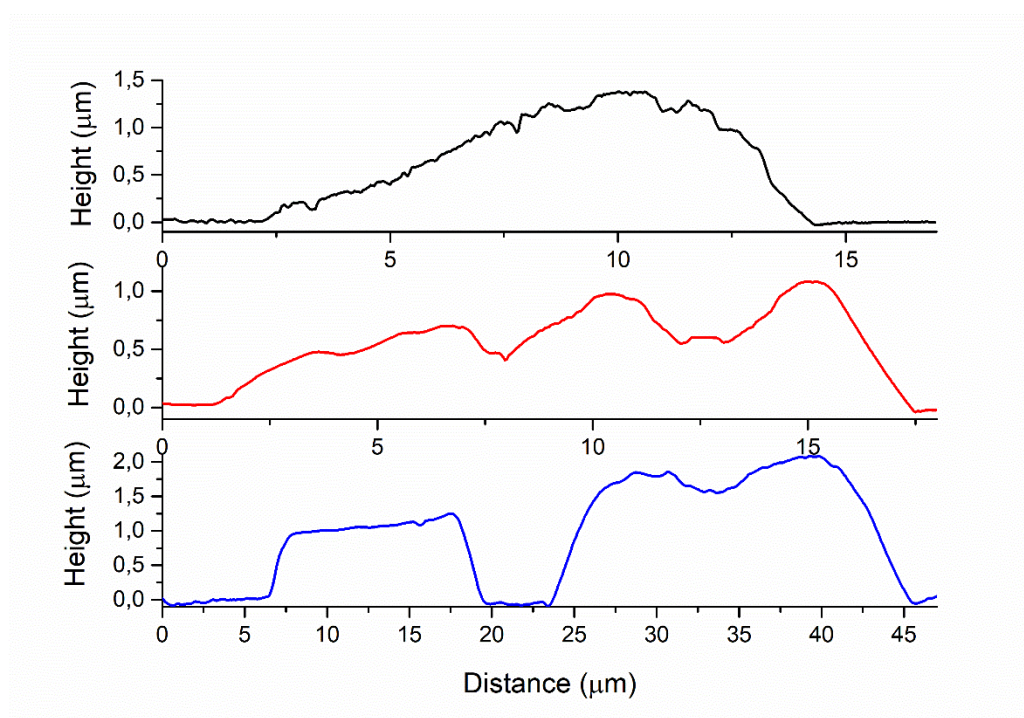


Figure S 10. AFM cross-section profiles of complexes: Fe(II) (black), Co(II) (red) and Zn(II) (blue) measured at marked places.

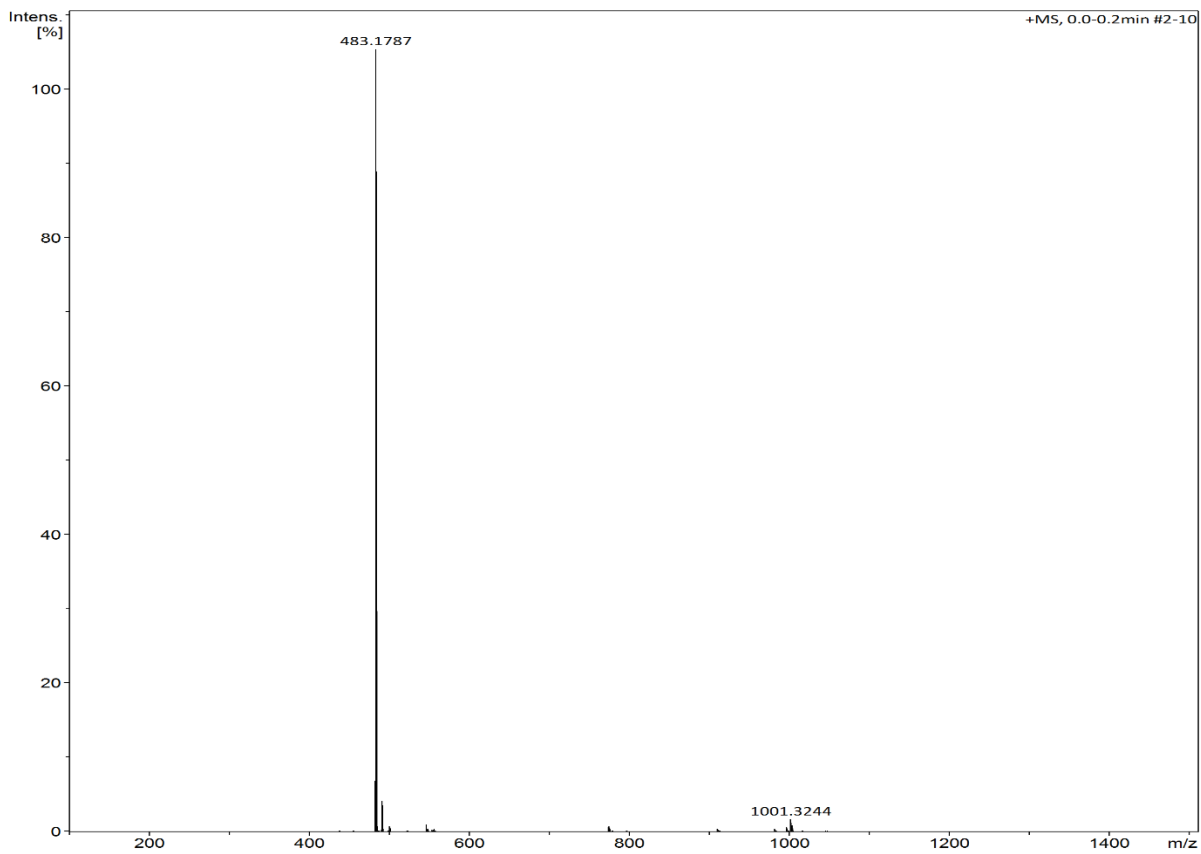


Figure S11. HR-ESI-MS spectrum of Fe(II) complex.

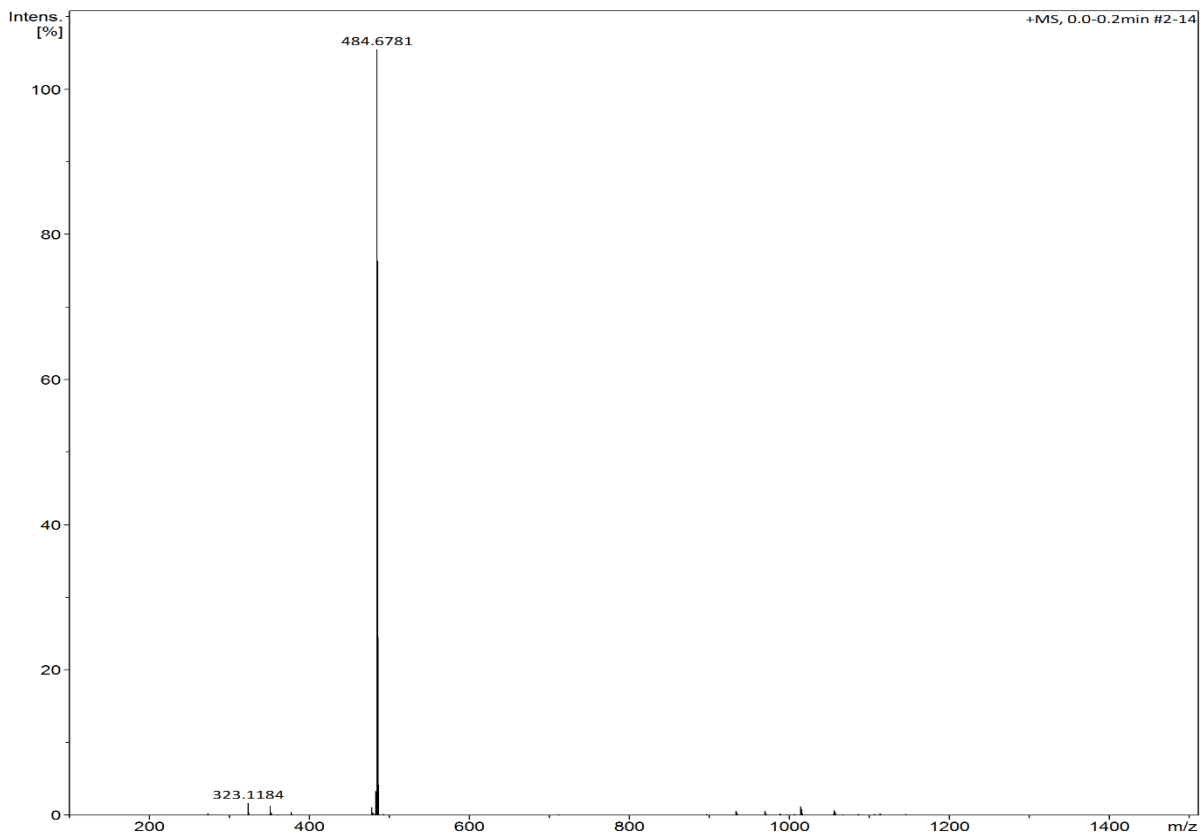


Figure S12. HR-ESI-MS spectra of Co(II) complex.

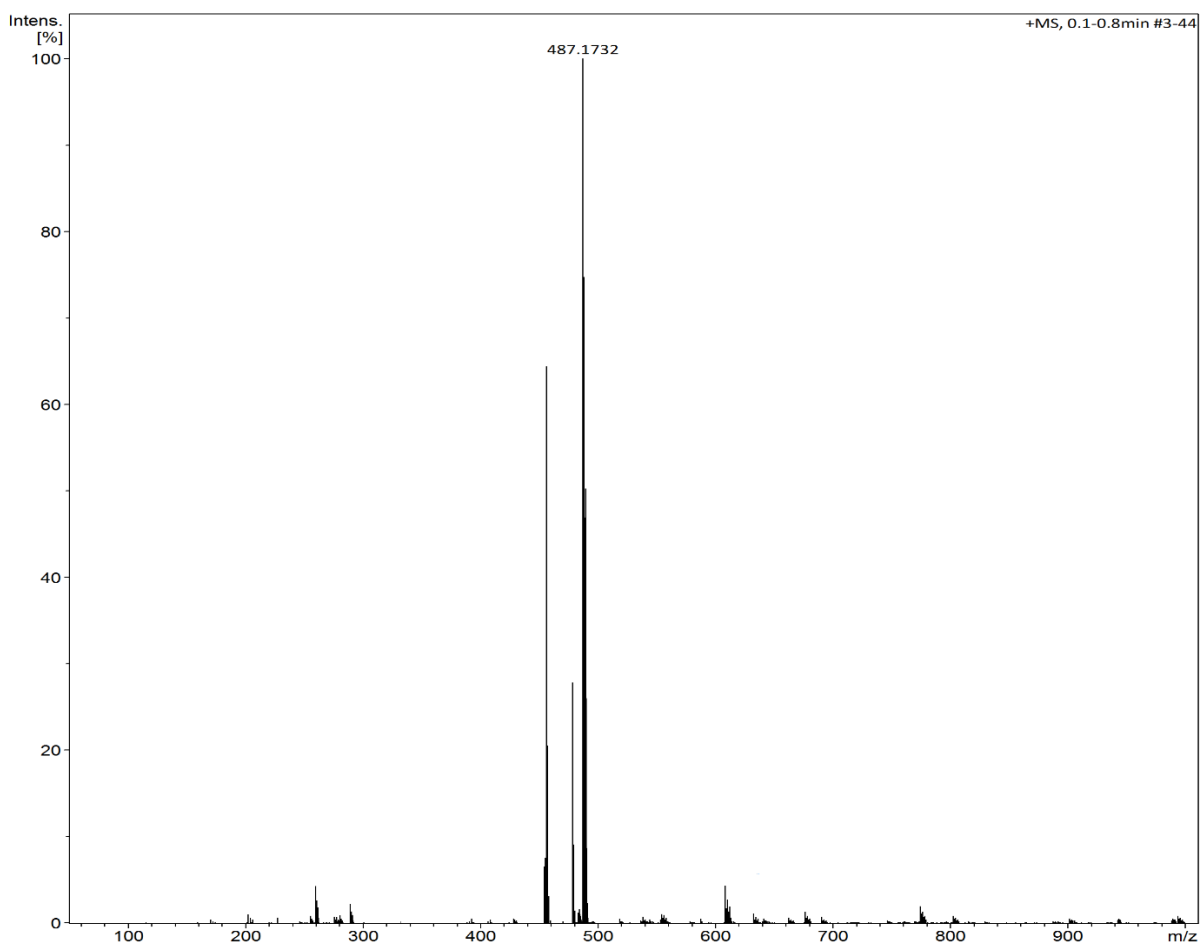


Figure S13. HR-ESI-MS spectra of Zn(II) complex.

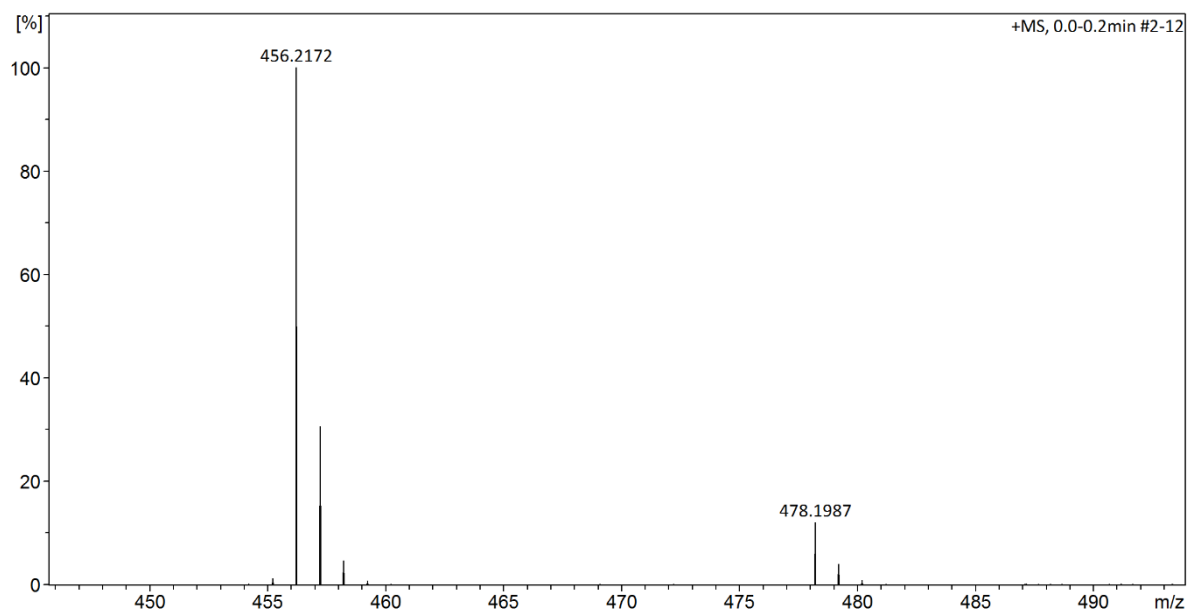


Figure S14. HR-ESI-MS spectra of ligand L.

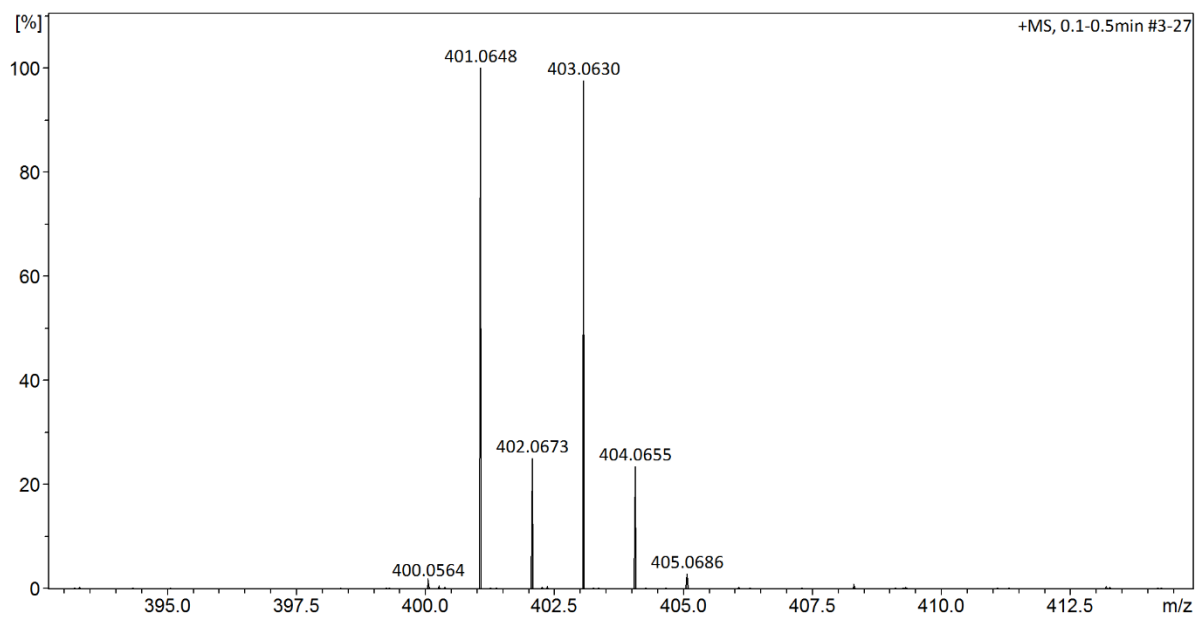


Figure S15. HR-ESI-MS spectra of compound **A**.

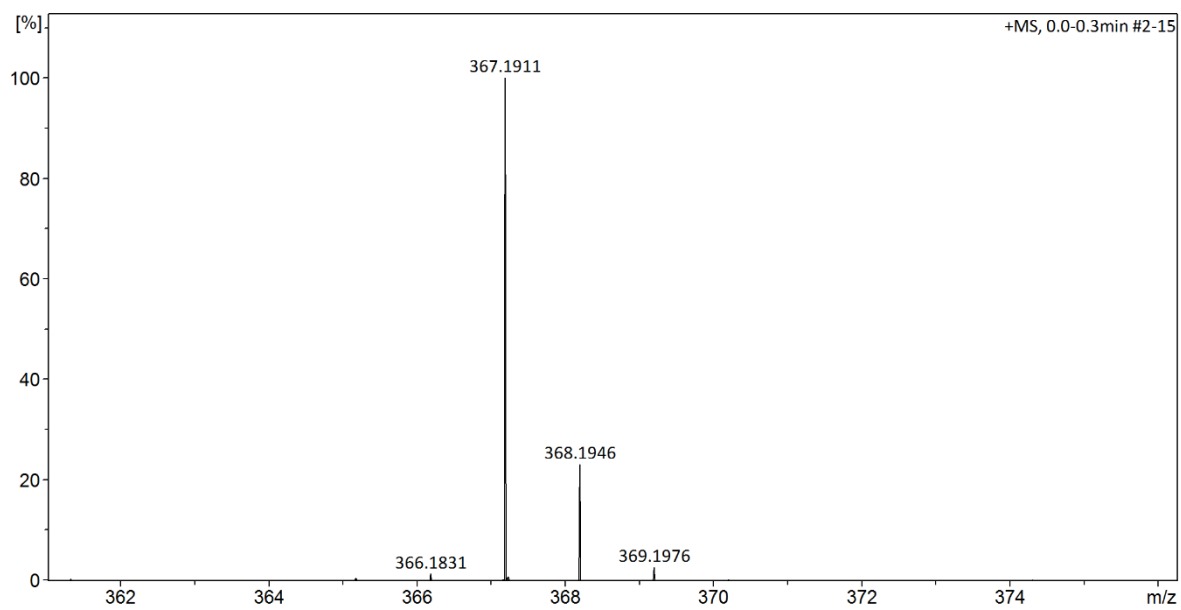


Figure S16. HR-ESI-MS spectra of compound **B**.

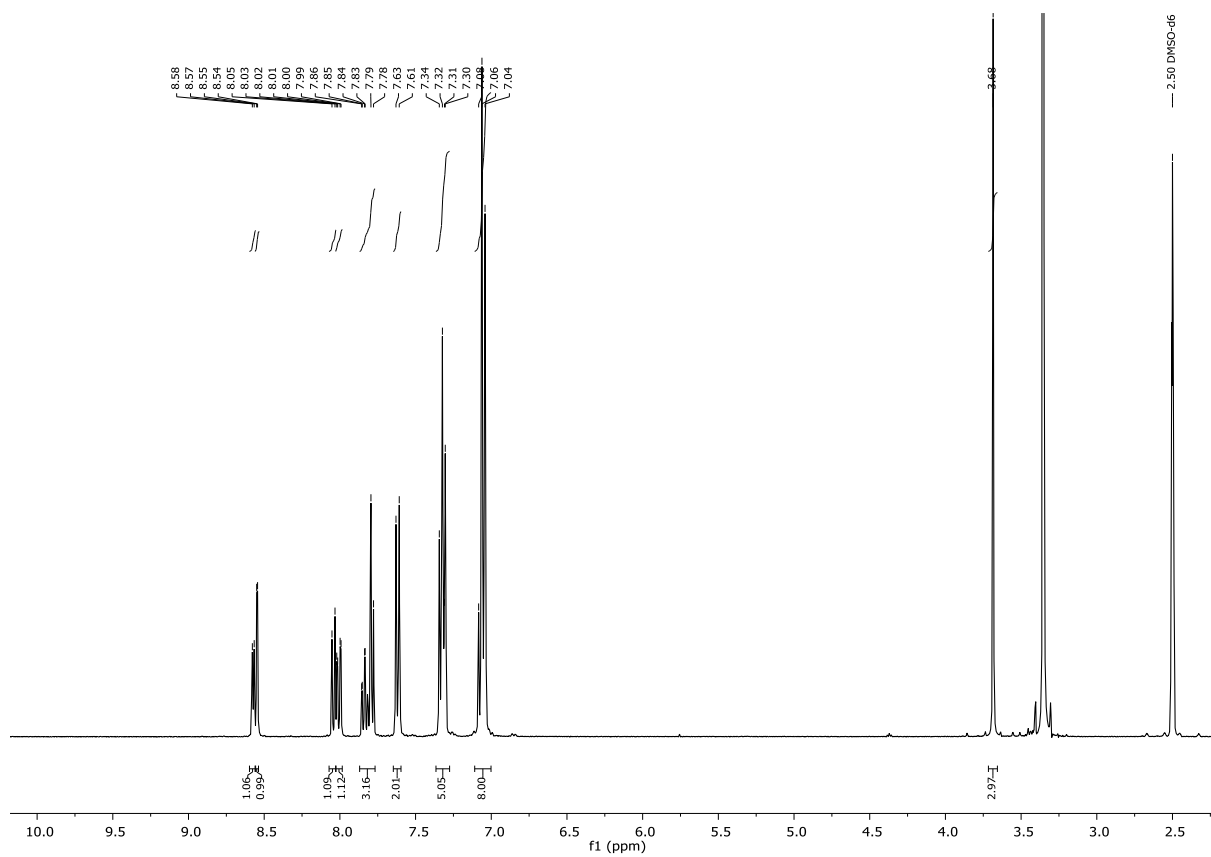


Figure S17. ^1H NMR spectra of ligand **L** in d_6 -DMSO.

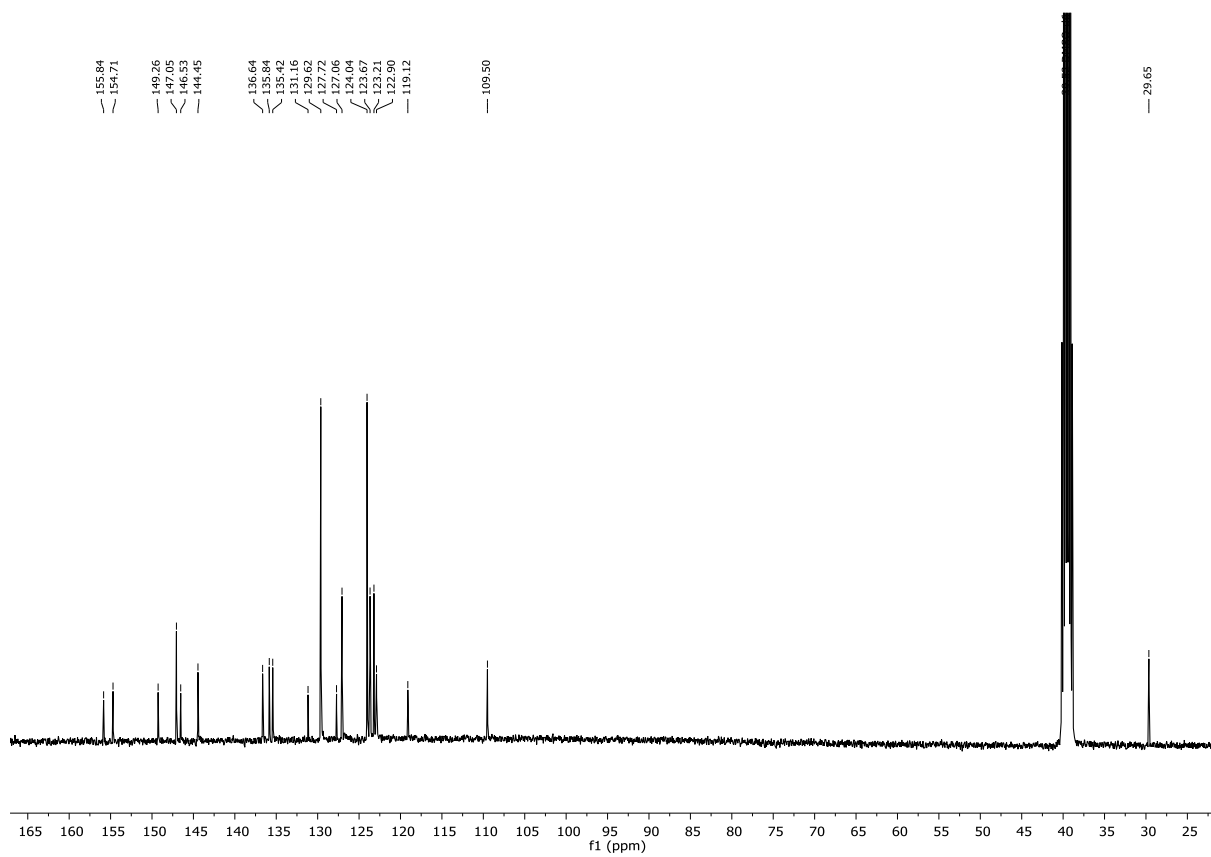


Figure S18. ^{13}C NMR spectra of ligand **L** in d_6 -DMSO.

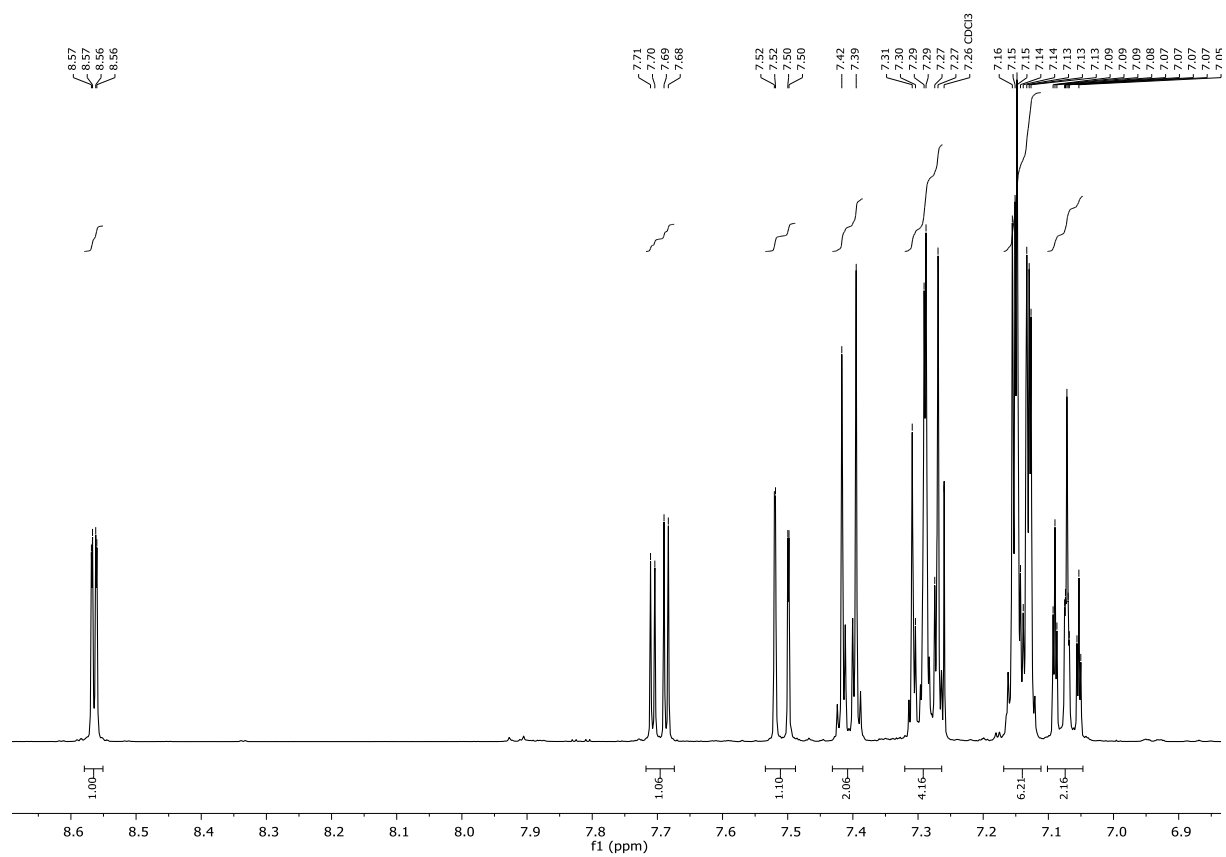


Figure S19. ¹H NMR spectra of compound **A** in CDCl₃.

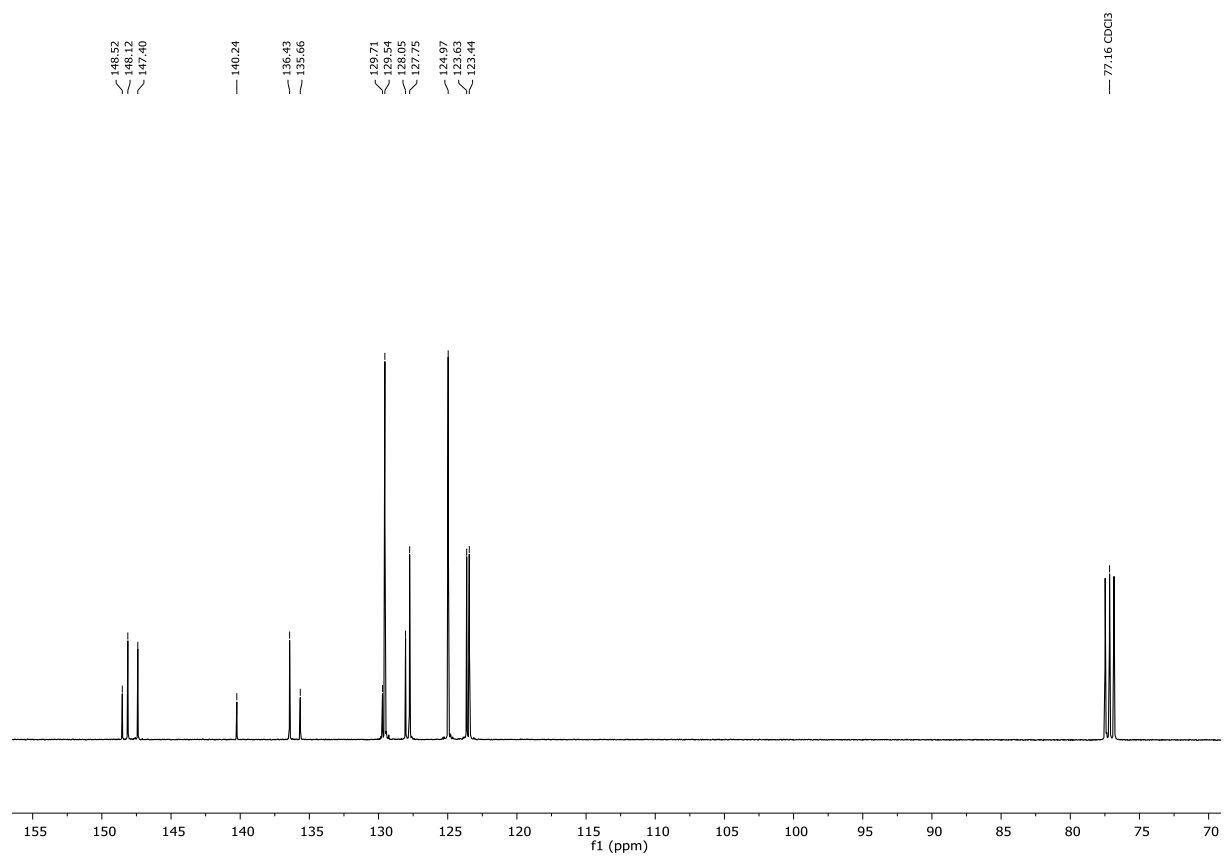


Figure S20. ¹³C NMR of compound **A** in CDCl₃.

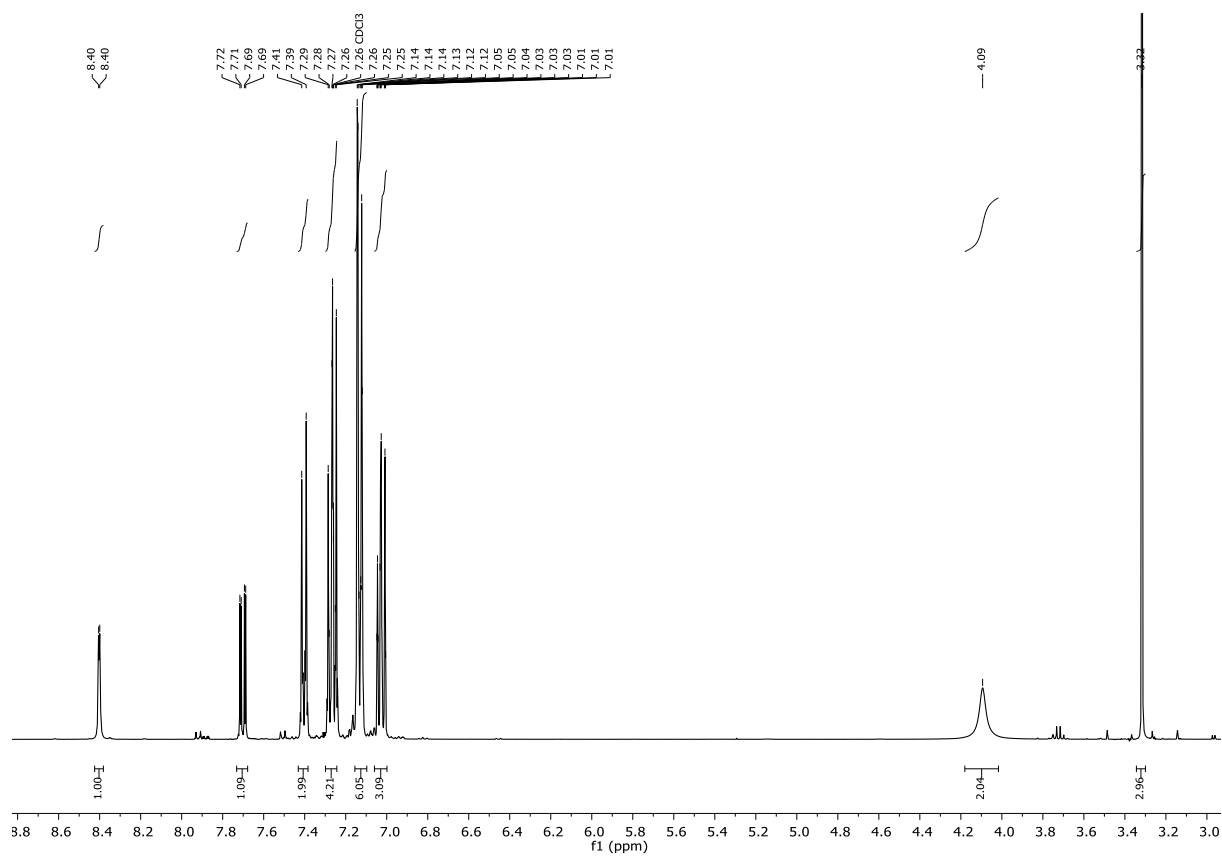


Figure S21. ^1H NMR spectra of compound **B** in CDCl_3 .

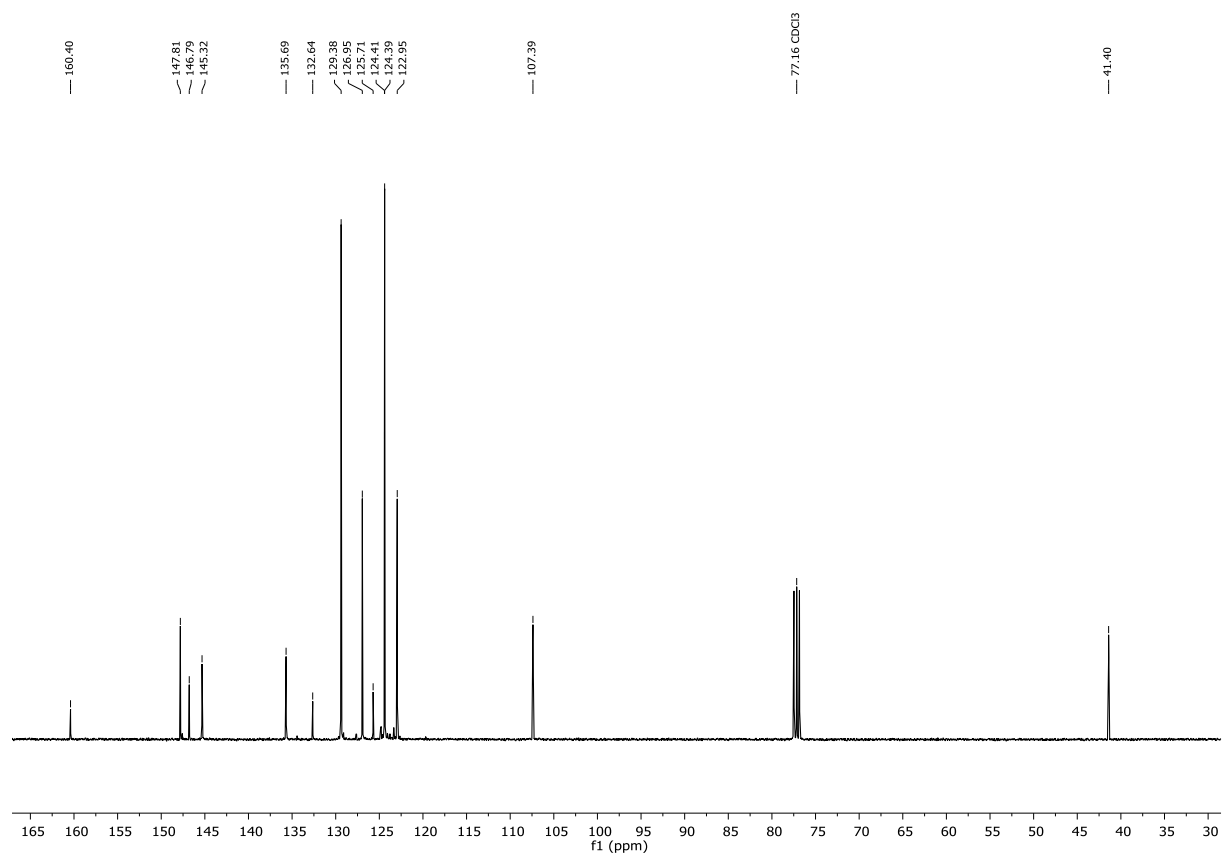


Figure S22. ^{13}C NMR spectra of compound **B** in CDCl_3 .